# Temperature stable 980 nm InGaAs/GaAsP vertical cavity surface emitting lasers for short-reach links

FATEN ADEL ISMAEL CHAQMAQCHEE*
*Department of Physics, Faculty of Science and Health, Koya University, Koya KOY45, Kurdistan Region, Iraq*

InGaAs/GaAsP based quantum well vertical cavity surface emitting lasers (VCSELs) operating in 980 nm are of great interest for optical interconnect applications to offer low cost and low power consuming light source. The devices are based on standard top and bottom AlGaAs distributed Bragg reflectors (DBRs) with high reflectivity. Static characteristics and modulation response were studied to observe thermal stability at high temperature short-reach optical links. Experimental results including an optical output power-current-voltage (*LIV*) and the spectral emission were performed with an oxide aperture diameter of 6 micrometers at temperature between 15 and 85 degrees Celsius. A maximum small-signal modulation bandwidths exceeding 22 gigahertz at an ambient temperature of 25 degrees Celsius has been reported.

## 1. Introduction

Vertical cavity surface emitting lasers (VCSELs) have recognized as key components in short-reach multimode fiber (MMF) links and mainly is used in optical interconnects (OIs) data centers and in super-computers for high modulation bandwidth and energy efficient light sources [1,2]. In addition to their modulation bandwidth and high speed performance characterization, VCSEL link have advantages of low fabrication cost, long−term system reliability, high temperature stability [3,4,5]. The main challenge with 980 nm VCSEL, the internal operating VCSEL can reach greater than 85 ℃ for such applications. The VCSEL geometries gives also significant advantages compared to the traditional edge emitter lasers (EELs) including ease to fabricate in arrays, support on wafer testing, low power consumption, low threshold current, optical coupling and less expensive wafer-scale manufacturing and testing [6,7]. The thermal behaviors of the VCSEL are varied than in the EEL, where the recombination of carriers in the active region and the Joule heating are the most heat source in VCSELs [8]. Additionally, the VCSEL devices have high electrical contact resistance and high output power comparing to the EELs as a result of their small top contact area and high reflectance band of distributed Bragg reflectors (DBRs) mirrors. The major problem with such VCSEL devices is abnormally high resistance in the upper of quarter wavelength stacks. The DBRs needed to have low resistance to allow the current injection and reduce the carrier heating in the quantum wells (QWs) [9]. The VCSEL with two-mesa structure have ability to combine with low electrical capacitance and high thermal conductance [10-12]. VCSELs at short wavelengths emission are formed from compressively strained InGaAs multiple quantum wells (QWs) lattice matched to GaAs based structure and surrounded by GaAs, AlGaAs or GaAsP barrier layers to achieve high differential gain, better thermal conduction and lower parasitics [13]. High speed VCSEL devices has been motivated by the market demand for high modulation bandwidth, as a result of demonstrating 850 nm VCSELs at room temperature operation at the bit rates up to 40 Gbit/s [14-16]. Room temperature 980 nm VCSELs demonstrated greater than 20 GHz bandwidth based InGaAs/GaAs QWs, and able to work at bit rates as high as 44 Gbit/s [17], and top emitting VCSEL operates with small signal modulation bandwidths of up to 26 GHz at up to 52 Gb/s [18]. In addition to the short wavelength VCSELs devices, VCSELs at wavelength of 990 nm, 1015 nm, 1040 nm, 1065 nm, and 1090 nm is achieved error-free transmission at 56 Gb/s by forming four 1×6 VCSEL arrays [19]. Error-free transmission over 2 km is demonstrated for a 1060 nm single-mode VCSEL at bit rates up to 40 Gb/s [20].

In this work, we have focused on a temperature dependence of 980 nm VCSEL at fixed oxide aperture diameter of ø~6 μm. Static characteristics with an estimated oxide aperture diameters ranging from ∅~ 6 to 19 μm at temperature of 25 ℃ is measured. This gives information on temperature insensitivity of VCSELs performance, including light output power-current-voltage (LIV), differential resistance (dR), wall plug efficiency (WPE) and optical emission spectra measurements. The devices with the oxide aperture diameter of ∅~ 6 μm at 25°C is designed to reduce the order modes with the current confinement profile. Thus, highly thermal stability of epitaxial 980 nm VCSELs to reach maximum bandwidths between (~20−25 GHz) is investigated.

## 2. Methodology

High speed vertical cavity surface emitting lasers (VCSELs) was designed for short reach optical interconnect systems in the ambient temperature [21]. The VCSEL structure as illustrated in Fig.1 (a) is top-emission and their layers are grown on each other on a GaAs substrate using metalorganic chemical vapor deposition (MOCVD) growth reactor [22]. The reflector mirrors made up of several quarter wavelengths thick layers of alternating high and low indices refractive forming the distributed Bragg reflectors (DBRs) stack. VCSELs use grading and doping schemes for p- and n-type DBRs to reduce their thermal resistance and optical absorption. The bottom n-DBRs employs 37−periods n−doped $Al_{0.9}Ga_{0.1}As$/GaAs DBRs and the top 20.5-periods p-DBRs contains two 20 nm thick $Al_{0.98}Ga_{0.02}As$ layers before oxidation layers for electrical and optical confinements.
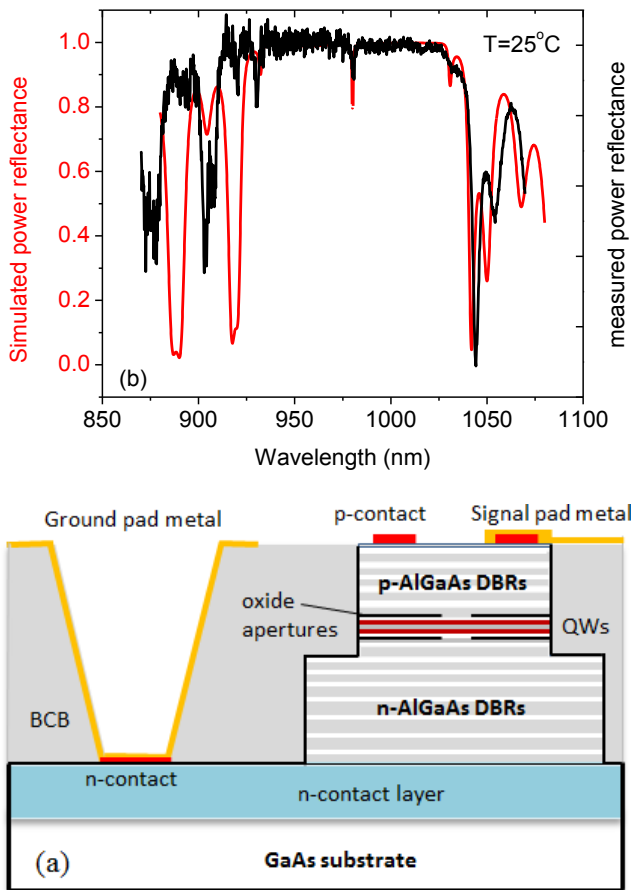


*Fig. 1. (a) Cross-sectional view to illustrate modulated oxide-confined high-speed VCSELs, (b) Stimulated and measured power reflectance of the wafer from which the 980 nm VCSEL was made at room temperature (color online)*

Stimulated with program and measured power reflectances are plotted in Fig.1 (b), where the reflectivity of these mirrors is typically in the range between 99.7 to 99.9%, the light oscillates perpendicular to these layers and escapes through the top or bottom of the device. The $1.5−\lambda$

thick cavity utilizes five strained $In_{0.22}Ga_{0.78}As$ quantum wells (QWs) by $Ga_{0.9}AsP_{0.1}$ barriers for high differential gain. A GaAs ohmic contact and buffer layer of 1.58 μm thick are just below of bottom n-DBRs. Besides, VCSELs was fabricated through numerous complex processing steps including E-beam evaporation and contact metallization, dry etching, selective wet oxidation and e−beam lithography to define a circular ring in the center of the VCSEL mesas. The double mesa high speed VCSELs were presented in a Unit Cell within a 16 rows × 15 columns array of 240 VCSELs, where the devices have the same top mesa diameter but with different bottom mesa diameters up to 400 μm for high power study. Geometrical contacts of a double mesa VCSELs structure and their operation array can be found elsewhere [23].

## 3. Results and discussion

Static characterization for 980 nm VCSELs is measured and evaluated using home built automated wafer mapping system. At room temperature, optical output power, current and voltage (*LIV*) data obtained from VCSEL of an oxide aperture diameter from ø~6 μm (Row0 ColumnB) into ø~8 μm (Row4 ColumnB) (increased by 0.5 μm), and between ø~8 μm and ø~19 μm (RowF ColumnB) (increased by 1 μm) are presented in Fig.2. Maximum optical output powers are about 0.75 (ø~6 μm) and 5.5 mW (ø~19 μm) at rollover current of 12 and 30 mA, respectively. The temperature dependence *LIV* between heat-sink between 25 and 85 ℃ are shown in Fig.3. Temperature stable, energy efficient and high bit rate oxide confined 980 nm VCSELs for optical interconnects is already reported in [24]. The maximum output power and the rollover operating current were decreased as the temperature increase from 15 to 85 ℃, and the resistance values for VCSELs at room temperature was expected to be high than the values of high temperatures [25].
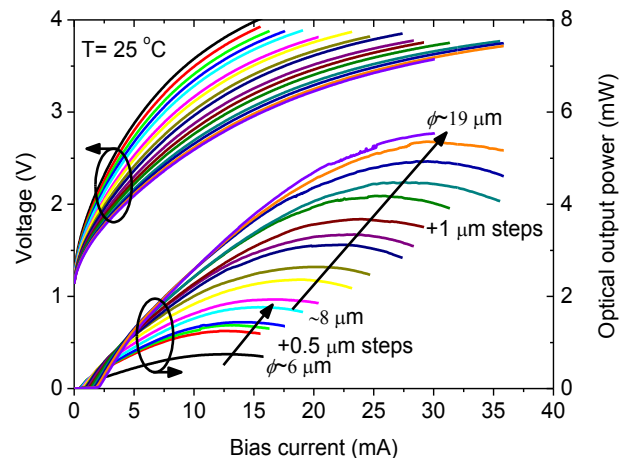


*Fig. 2. Static LIV characteristics of VCSEL wafer with an estimated oxide aperture diameters ranging from ø~ 6 (Row0) to 19 μm (RowF) at 25 ℃ (color online)*
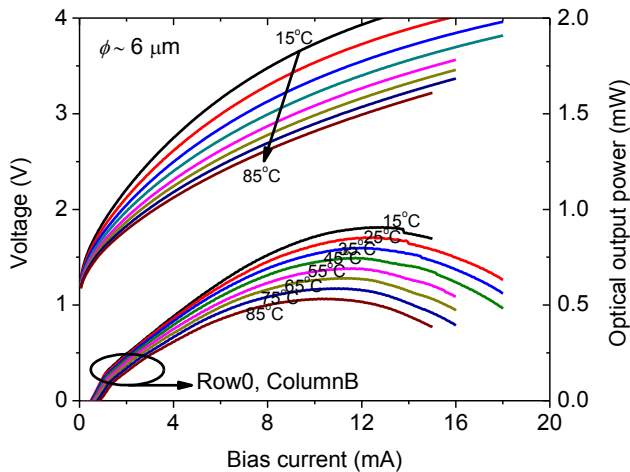
*Fig. 3. Static LIV charactaristics of VCSEL wafer with Ø~ 6 μm and temperature between 25 and 85 ºC (color online)*

Fig. 4 (a) shows the extracted threshold current, threshold power, wall plug efficiency (WPE) and optical output power from VCSEL of ø~6 μm as a function of temperature. An optical output powers at rollover are decreased from 0.93 to 0.53 mW at high temperature, while the threshold currents are increased from 0.47 mA at 15 ºC into 0.79 mA at 85 ºC. It is also observed that with decrease in threshold voltages, the threshold of optical output powers increases from 0.7 into 1.23 at 85 ºC. Generally, the threshold current decreases with decreasing oxide aperture diameters and a slight increase in threshold current is observed with temperature, and this increase is larger for smallest mesas diameters VCSELs as a results of their lower capacity to dissipate heat compared with larger mesas diameters VCSELs [26]. The power conversion efficiency (PCE) of optical output power / electrical power ($P_{opt}/P_{Ele}$) in at 15 and 85 ºC are about 7.5% and 4.9%, respectively. We extracted the WPE as $\Delta L/\Delta(I \times V)$ and the differential resistance (dR) as $\Delta V/\Delta I$ from *LIV* measurements at temperature from 15 to 85 ºC as shown in Fig.4(b). By increasing the bias current, the WPE and dR decrease. The dR is also decreases with temperature for ø~6 μm.



*Fig. 4. Static light-current-voltage (LIV) charactaristics of 980 nm VCSEL wafer with (a) an extracted threshold current, threshold power, maximum optical output power and power conversion efficiency of ø~6 μm (Row0) at various temperatures, and (b) WPE and dR with ø~6 μm at temperature of T~ 15 to 85 ºC (color online)*

The optical spectra measurements and the small signal modulation response setup used by here were previously described in detail [27]. The output light from VCSEL is coupled into a straight split fiber and then into an optical spectrum analyzer (OSA) Ando AQ6317C, to analysis optical spectra over wide wavelength ranges. Fig.5 shows the measured continuous wave (CW) optical emission spectra for multi-modes VCSELs of LP01, LP11 and LP21 modes with oxide aperture diameter of ø~6 μm (Row 0 Column B) under injected currents of 1.18 mA at temperature of 25 and 85 °C. The cavity resonance shift-rate is estimated to be around 0.062 nm/K for VCSELs with ø > 3.5 μm, and depends on the oxide aperture diameters [28]. Additionally, the VCSELs with smaller oxide aperture diameters suffer from larger thermal resistance [29].
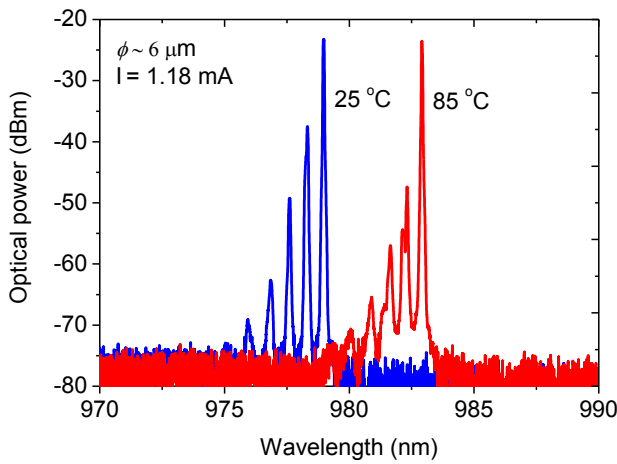


*Fig. 5. Emission spectra for a 980 nm VCSEL of ~6.0 μm at current bias of 1.18 mA at 25 and 85 °C (color online)*

The measured fundamental mode peak emission wavelength as a function of temperatures at applied bias current between 0.2 and 10 mA are depicted in Fig. 6.
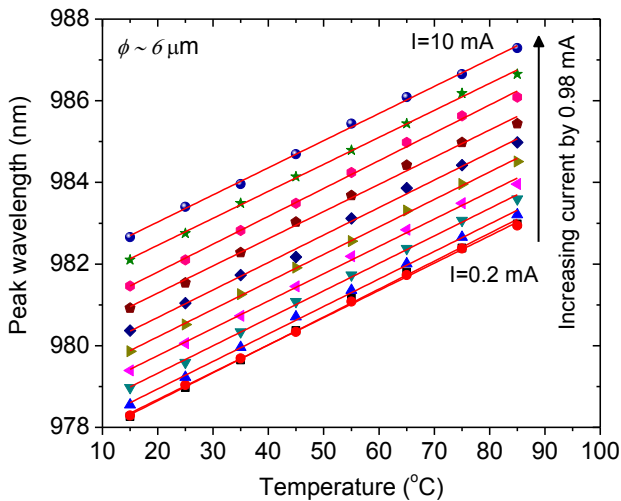


*Fig. 6. Fundamental mode peak emission wavelength as a function of temperatures of VCSELs at bias current between I= 0.2 and I=10 mA and fixed of Ø ~6.0 μm (color online)*

By fitting the data with a straight line, VCSEL peak wavelength is linearly increased with temperatures at applied bias currents of 0.2, 1.18, 2.16, 4.14, 4.12, 5.1, 6.08, 7.06, 8.04, 9.02 and 10 mA with slopes data of $\Delta\lambda/\Delta T$ are about 0.06837, 0.0668, 0.06735, 0.06727, 0.06692, 0.06732, 0.06727, 0.6656, 0.0682, 0.06607 and 0.06643 nm/K, respectively. The linear fit gives the value of the cavity resonance wavelength shift rate versus temperature $\Delta\lambda/\Delta T$.

In Fig. 7 we show emission spectra of 980 nm VCSELs with an oxide aperture diameter of ~6.0 μm at forward bias currents between 0.6 and 8.0 mA. The inset easily identify the spectral modes of LP01, LP11 and LP21 as a function of the forward bias electrical power (I×V) for the 980 nm VCSELs. By fitting the data with a straight line, the wavelengths of the LP01, LP11, and LP21 modes at zero electrical power called cold cavity modes.
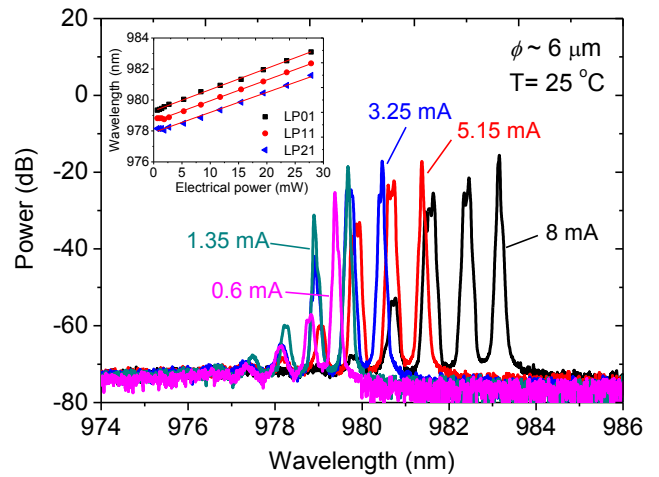


*Fig. 7. Emission wavelength at various biases current and at 25 °C, the inset show room temperature emission wavelength of LP01, LP11 and LP21 modes versus CW electrical power of current× voltage (I×V) (color online)*

The room-temperature small-signal electrical modulation response ($|S_{21}|$) measurements were performed using a 50 MHz - 40 GHz HP 8722C network analyzer (NWA) with the light from the VCSEL coupled to a multimode optical fiber (MMF) [30]. The values of $f_{-3dB}$ extracted from the small signal response $S_{21}$ measurements for VCSELs against driving current at a heat sink room temperature. The bandwidth is depends on the injection current that observed between 0.5 to 28 mA as shown in Fig. 8. At room temperature of 25 °C, the smaller aperture VCSEL reaches a modulation bandwidth of 22 GHz while the larger aperture VCSEL has a maximum modulation bandwidth of greater than 22 GHz.
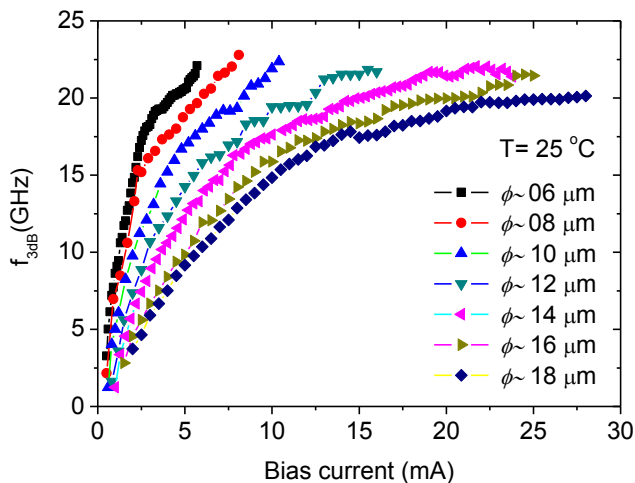
*Fig. 8. The –3 dB modulation bandwidth frequency $f_{3dB}$ against bias current with VCSELs aperture diameters ranging from $\emptyset$ ~6 to 18 μm at temperature of 25 ºC (color online)*

## 4. Conclusion

The performance of top emitting 980 nm VCSELs at various temperatures is demonstrated to achieve a thermal stability at high temperatures for future short reach optical interconnects (OIs), particularly in high-performance computers (HPC) applications. VCSELs with high modulation bandwidth of $\geq$ 22 GHz of smaller aperture diameter at $\emptyset$ ~ 6 μm and at threshold current of ~6 mA is presented, with corresponding emission spectra for multi-modes VCSELs of LP01, LP11 and LP21 modes. The demand for VCSEL devices in markets and companies were increased rapidly, following the development of institutions research, optimizing VCSEL performance and improving output power in the near future.

## References

[1] M. A. Taubenblatt, J. Lightwave Technol. **30**(4), 448 (2012).
[2] C. DeCusatis, IEEE J. of Lightwave Technol. **32**(4), 544 (2014).
[3] N. Haghighi, R. Rosales, G. Larisch, G. Marcin, L. Frasunkiewicz, T. Czyszanowski, J. A. Lott, Proc. SPIE **10552**, 1 (2018).
[4] N. Haghighi, J. A. Lott, Materials **14**(397), 1 (2021).
[5] F. A. I. Chaqmaqchee, J. Optoelectron. Adv. M. **22**(7-8), 339 (2020).
[6] A. Larsson, IEEE J. Sel. Top. Quantum Electron **17**(6), 1552 (2011).
[7] F. A. I. Chaqmaqchee, Aro-the Scientific Journal of Koya University **8**(1), 107 (2020).
[8] H. Li, P. Wolf, X. Jia, J. A. Lott, D. Bimberg, Appl. Phys. Lett. **111**(24), 243508 (2017).
[9] F. A. Chaqmaqchee, Aro-the Scientific Journal of Koya University **9**(1), 89 (2021).
[10] Y. Ou, J. S. Gustavsson, P. Westbergh, A. Haglund, A. Larsson, A. Joel, IEEE Photon. Technol. Lett. **21**(24), 1840 (2009).
[11] P. Moser, Energy-Efficient VCSELs for Optical Interconnects. Berlin, Germany: Springer, 2016.
[12] A. N. Al-Omari, G. P. Carey, S. Hallstein, J. P. Watson, G. Dang, K. L. Lear, IEEE Photonics Technology Letters **18**(11), 1225 (2006).
[13] S. B. Healy, E. P. O'Reilly, J. S. Gustavsson, P. Westbergh, A. Haglund, A. Larsson, A. Joel, IEEE J. Quantum Electron **46**(4), 506 (2010).
[14] N. Haghighi, J. Lavrencik, S. E. Ralph, J. A. Lott, paper TuE3-3, 24th OptoElectronic and Communications Conference (OECC), Fukuoka, Japan (2019).
[15] M. Gębski, P.-S. Wong, M. Riaziat, J. A. Lott, Journal of Physics Photonics **2**(3), 1 (2020).
[16] P. Westbergh, E. P. Haglund, E. Haglund, R. Safaisini, J. S. Gustavsson, A. Larsson, Electron. Lett. **49**(16), 1021 (2013).
[17] Y-C. Chang, L. A. Coldren, IEEE Journal of Selected Topics in Quantum Electronics **15**(3), 704 (2009).
[18] E. Haglund, P. Westbergh, J. S. Gustavsson, E. P. Haglund, A. Larsson, Electron. Lett. **51**, 1096 (2015).
[19] Y-C. Chang, L. A. Coldren, IEEE Journal of Selected Topics in Quantum Electronics 15, (2009).
[20] B. Wang, W. V. Sorin, P. Rosenberg, L. Kiyama, S. Mathai, M. R. T. Tan, Journal of Lightwave Technology **38**(13), 3439 (2020).
[21] E. Simpanen, Johan S. Gustavsson, Anders Larsson, Magnus Karlsson, Wayne V. Sorin, Sagi Mathai, Michael R. Tan, Scott R. Bickham, Journal of Lightwave Technology **37**(13), 2963 (2019).
[22] C.-C. Shen, T.-C. Hsu, Y.-W. Yeh, C.-Y. Kang, Y.-T. Lu, H.-W. Lin, H.-Y. Tseng, Y.-T. Chen, C.-Y. Chen, C.-C. Lin, C.-H. Wu, P.-T. Lee, Y. Sheng, C.-H. Chiu, H.-C. Kuo, Nanoscale Research Letters **14**(276), 1 (2019).
[23] F. A. Chaqmaqchee, Aro-the Scientific Journal of Koya University **9**(2), 112 (2021).
[24] H. Li, P. Wolf, P. Moser, G. Larisch, J. A. Lott, D. H. Bimberg, IEEE Journal of Selected Topics in Quantum Electronics **21**(6), 405 (2015).
[25] N. Haghighi, P. Moser, J. A. Lott, Power, IEEE Journal of Selected Topics in Quantum Electronics **25**(6), (2019).

[26] R. Rosales, M. Zorn, J. A. Lott, IEEE Photonics Technology Letters **29**(23), 2107 (2017).

[27] N. Haghighi, P. Moser, J. A. Lott, Journal of Lightwave Technology **38**(13), 3387 (2020).

[28] H. Li, P. Wolf, P. Moser, G. Larisch, A. Mutig, J. A. Lott, D. H. Bimberg, IEEE Journal of Quantum Electronics **50**(8), 613 (2014).

[29] T. Flick, K.H Becks, J. Dopke, P. Mättig, P. Tepel, Journal of Instrumentation **6**, 1 (2011).

[30] F. A. I. Chaqmaqchee, J. A. Lott, OSA Continuum 3(9), 2602 (2020).

_____

*Corresponding author: faten.chaqmaqchee@koyauniversity.org